Quantum Optics and Laser 2021/22
Report 1 - Arecchi's Wheel
Prof. Paolo Villoresi

Samuele Piccinelli
(Dated: 28 October, 2021)

An understanding of photon-number statistics is important for applications such as the reduction of noise in weak images and the optimisation of optical information transmission [1]. The statistical distribution of photons depends on the nature of the light source: we differentiate between the two most important cases of coherent and thermal light sources. In this report we show the analysis of the statistical distribution of photons from a coherent laser source and a comparison with the distribution from an incoherent source via photon counting technique. The experimental setup is based on Arecchi's wheel [2]. The aim is to verify the Poisson and Bose-Einstein statistics of photons emitted from the coherent and thermal source respectively.

1 Theoretical background

For photon streams the classical intensity $I(\mathbf{r}, t)$ determines the mean photon flux density $\phi(\mathbf{r}, t)$ through the relation $\phi = I/h\bar{\nu}$: the fluctuations around the mean of this value, i.e. the statistical properties of the arrival time of the photons, are determined by the nature of the source emitting the photons. Given a source of optical power P, the arrival of photons may be regarded (under certain conditions) as the independent occurrences of a sequence of random events at a rate equal to the photon flux - in the general case a function of time, $\Phi = P(t)/h\bar{\nu} \propto P(t)$. The optical power may be deterministic in the case of **coherent** light or a time-varying random process as with **thermal** light. We analyse briefly these two possible scenarios.

Coherent light. Coherent light is characterised by a source with constant optical power $P(t) = P$ and with corresponding mean photon flux $\Phi = P/h\bar{\nu}$. The mean photon number is given by

$$\bar{n} = \Phi T = PT/h\bar{\nu} \tag{1}$$

with T being the **counting time** and n the number of detected photons called the **photon number**. The photon number distribution $p(n)$ follows a **Poisson** distribution of the form

$$p(n) = \frac{\bar{n}^n \exp(-\bar{n})}{n!},\ n \in \mathbb{N} \tag{2}$$

and can be derived under the assumption that the photon registrations are statistically independent events. The mean of the Poisson distribution is $\bar{n}$ and its variance is equal to its mean, $\sigma_n^2 = \bar{n}$. The higher order moments of skewness and kurtosis are given by $s = 1/\sqrt{\bar{n}}$ and $k = 1/\bar{n}$ respectively. Moreover, the photon-number-based signal-to-noise ratio (SNR) is given for a Poisson photon number statistics by $\text{SNR} = \bar{n}$, i.e. it increases linearly with the mean photon number.

Thermal light. When the photon arrival times are not independent, as it is the case for thermal light, the photon-number differs from the Poisson statistics. By considering statistical nature of the probability distribution of the energy levels in a thermal light source (i.e. a so called **optical resonator**) it can be shown that the probability distribution for the number of photons n

can be rewritten in terms of the mean photon number $\bar{n}$ as

$$p(n) = \frac{1}{\bar{n}+1}\left(\frac{\bar{n}}{\bar{n}+1}\right)^n, \; \bar{n} = \frac{1}{\exp(h\nu/kT)-1} \tag{3}$$

where ν is the frequency of the optical resonator, T the temperature and k Boltzmann's constant. In Eq. (3) $p(n)$ is referred to as the Bose-Einstein distribution and is known in probability theory jargon as geometric distribution. The photon number distribution for thermal light $p(n)$ decreases monotonically from $n = 0$ and is far broader than the one for coherent light.
Having defined for simplicity $l \equiv \frac{1}{\bar{n}+1}$, $p(n) = l(1-l)^n$, for the higher order moments it holds $\sigma_n^2 = \frac{1-l}{l^2}$, $s = \frac{2-l}{\sqrt{1-l}}$ and $k = \frac{l^2}{1-l} + 9$, where $\bar{n}$ is the photon number mean.
The photon-number fluctuations are far greater than those of the Poisson distribution: this large variability is consistent with the random nature of thermal light. This is further highlighted by the SNR, which is given by $\text{SNR} = \frac{\bar{n}}{\bar{n}+1}$: since in this case $\text{SNR} < i \; \forall n$, thermal light is generally too noisy to be used for the transmission of information.

PHOTON NUMBER STATISTICS. To characterise the random variable n, the moments of its distribution $p(n)$ are used. These are computed from the empirical data through

$$\bar{n} = \sum_{n=0}^{\infty} n \cdot p(n) \tag{4}$$

$$\sigma_n^2 = \sum_{n=0}^{\infty} (n-\bar{n})^2 \cdot p(n) \tag{5}$$

$$s_n = \sum_{n=0}^{\infty} (n-\bar{n})^3 \cdot p(n) \tag{6}$$

$$k_n = \sum_{n=0}^{\infty} (n-\bar{n})^4 \cdot p(n) \tag{7}$$

with s_n and k_n being the empirical skewness and kurtosis respectively.

2 EXPERIMENTAL SETUP

The experimental setup consists of:

- A single-photon avalanche diode (SPAD);
- An amplitude-stabilised single-mode He-Ne laser;
- A sandpaper wheel, able to rotate on its central axis;
- A single mode fiber to redirect the photons towards the detector.

The coherent radiation is approximated by the laser. However, it is possible to simulate the behaviour of a thermal source by altering the spatial and temporal coherence of the generated light beam by interposing a time-varying corrugated surface between the source and detector (the rotating sandpaper wheel). In fact, when the wheel is set into rotation, its surface can be seen as a series of independent emitters. The scattered light can be more or less intense depending on the surface that instant by instant is lit by the laser: this behaviour mimics the essence of a thermal source with a fixed average value but a varying configuration in time.
In case of resting wheel, the irregular surface is comparable to a dimming element and does not affect the nature of the emitted light.

3 DATASET

Ten datasets are taken for each configuration of resting and spinning wheel: the acquisition time is $\approx 15.26\,\mathrm{s}$ for the former and $\approx 24.11\,\mathrm{s}$ for the latter. The difference in the acquisition time is due to the experimental setup: for the case of the spinning wheel in fact, part of the photons are scattered away. This portion of emitted light does not reach the detector and is thus not acquired. The time tags are recorded on a single channel (CH1) in machine units (m.u.) and for the conversion to seconds it holds $1\,\mathrm{m.u.} \equiv 81\,\mathrm{ps}$.
Fig. 1 shows the difference distribution in time between the arrival of one photon and the previous one: the first 500 events have been represented for visual ease.
Events are not equidistant in time: although the distribution of the time difference looks random, most of events are related to a time difference of $\sim 100\,\mathrm{km.u.}$ and only few events have a time difference larger than $\sim 200\,\mathrm{km.u.}$ for the resting wheel. In contrast, for the spinning wheel, the maximum distance value is more than double with respect to the previous one: the time difference distribution is in general shifted of about an order of magnitude and is more heterogeneous, consisting of a large portion of events with a short time distance. This is to be expected from a thermal source, which emits light with frequent and random change of phase between the photons: clicks can thus happen very close to one another.

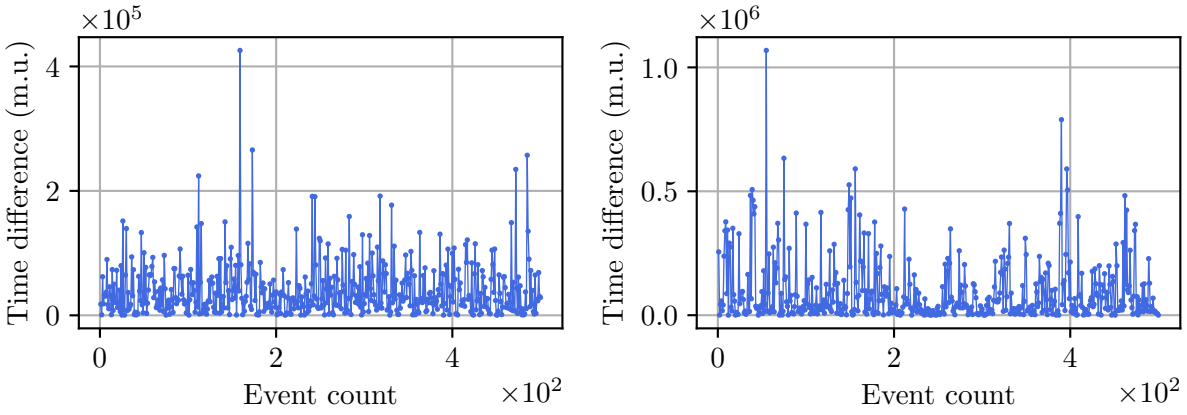

(a) Resting wheel.

(b) Spinning wheel.

Figure 1: Time difference distribution in the two different configurations.

4 ERROR CORRECTION

The single photon counting module is subject to experimental errors due to its construction. In this section we analyse two of the most prominent effects and their causes. To this scope, a histogram of the time differences is constructed: in Fig. 2 the result is shown in semi-log scale. From the zoomed window it is clear that the trend for small time differences is not comparable from the rest of the data. This trend is attributable to the first effect we describe.

AFTERPULSING EFFECT. In counting experiments using photomultipliers and avalanche diodes that are operated in the photon counting (Geiger) mode, genuine output pulses may be followed by an **afterpulse**. The origin of this phenomenon and its characteristics depend on the detector type. For photomultipliers the most frequent cause for afterpulsing are ionised atoms of

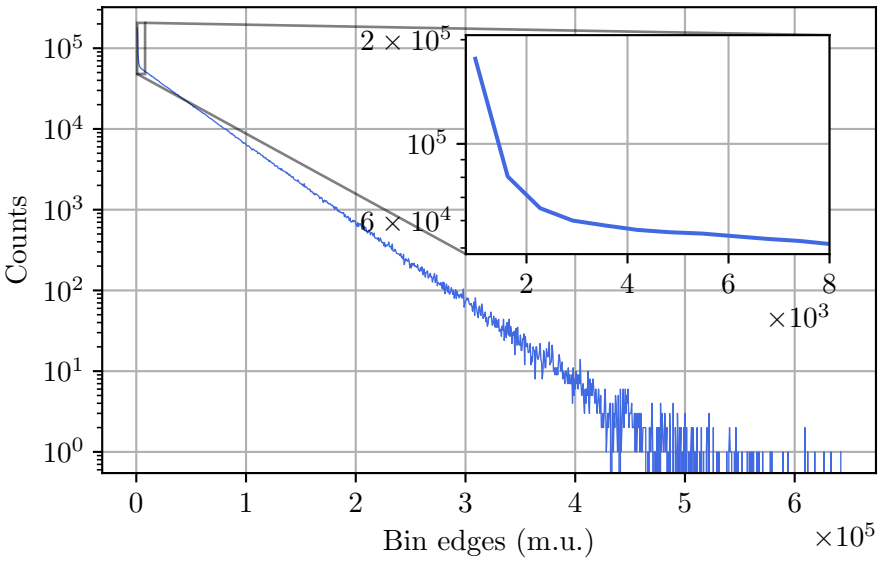

Figure 2: Histogram of the time differences in semi-log scale.

the residual gas that are accelerated towards the photo-cathode and generate delayed photoelectrons. In semiconductor avalanche diodes a primary photoelectron initiates a chain of ionisation that causes a breakdown pulse at the detector output. Some of the generated charge carriers are however temporally trapped in the junction depletion layer. When these carriers are released by thermal excitation, new free carriers are released by thermal excitation that can lead to after-pulses which are correlated with the initial event.
The probability of afterpulsing depends on many different parameters like material defects, temperature and operating conditions of the SPAD. For this reason only an estimate is given for the time τ_{ap} after which the counts are considered coming from actual events, keeping in mind that in practical applications one has to compromise between high count rates and a tolerable level of afterpulsing. It has been observed however that fluctuations of a few µs do not affect the following analysis. The threshold is therefore set at $\approx 105\,\text{ns}$ which corresponds to a $\sim 5\%$ rejection of the total experimental data.

DEAD TIME. When considering an avalanche diode at a fixed operating bias voltage, after the detection of an event the detector will be insensitive to the impinging radiation because of inherent **dead time**. This means that the detector is inactive during a time τ_{dt} after a detected photon followed by an infinitesimal short transition to its full efficiency.
The detector is thus unable to show us any evidence that comes with an interval that comes shorter than $20 - 40\,\text{ns}$ (according to the SPCM-AQRH Series SPAD datasheet). This is consistent with what we observe: the first pulse after dead time is around 54 ns for the case of resting wheel.
Note that the shorter the dead time the more visible the afterpulsing effect.

Considering the qualitative approach used in this report, the errors on the estimates of the momenta obtained from the following analysis are shown without uncertainty and are only compared via percentage deviation with the theoretical values. Moreover, the poissonian errors on the histograms of the final probability distributions have shown to be up to 4 orders of magnitude smaller than the count and are thus neglected.

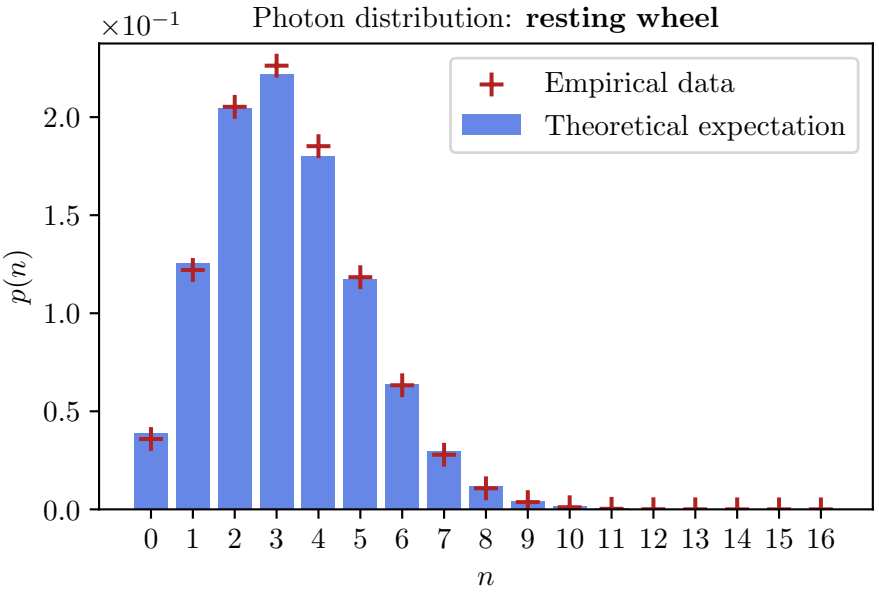

Figure 3: Photon distribution in case of coherent light (resting wheel configuration).

5 Analysis and discussion

Data were segmented into intervals of 12 µs and the number of photons collected in that period registered. The frequencies in each interval for each single dataset were consequently summed together to obtain the total frequency for the whole acquisition time. To obtain the expected probability distribution, the frequencies were normalised to the total photon count. The obtained results are shown in Fig. 3, up to the 16-photon count/interval bin.
In Table 1 we list the results computed with the formulae seen in Section 1.

M_i	M_i^{exp}	M_i^{th}	$\left(1 - \frac{M_i^{\text{th}}}{M_i^{\text{exp}}}\right)\%$
M_1	3.25	3.25	-
M_2	3.11	3.25	-4.7%
M_3	0.52	0.55	-7.4%
M_4	3.24	3.31	-2.2%

Table 1: Theoretical and experimental moments associated to the Poisson statistics in Fig. 3.

As it can be observed, the experimental values are in line with the theoretical ones: the percentage difference from the expected value is systematically negative. The distribution has a mean of around 3 photons in the considered interval, which is consistent with what was observed in Fig. 1.

An analogous analysis has been carried out for the case of the spinning wheel. Fig. 4 shows the obtained distribution, while in Table 2 the calculated moments are listed.
It can be observed that the expected value for the mean number of photons is indeed less than the one found in the case of coherent light, as mentioned in Section 3. In contrast with the Poisson

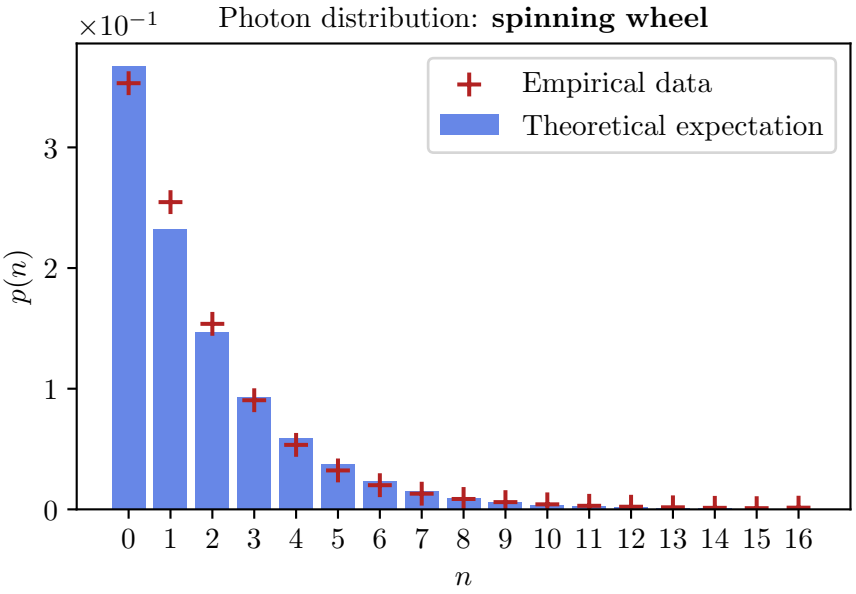

Figure 4: Photon distribution in case of incoherent light (spinning wheel configuration).

M_i	M_i^{exp}	M_i^{th}	$\left(1-\frac{M_i^{\text{th}}}{M_i^{\text{exp}}}\right)\%$
M_1	1.72	1.72	-
M_2	4.98	4.68	6.1%
M_3	2.36	2.05	13.0%
M_4	10.73	9.21	14.1%

Table 2: Theoretical and experimental moments associated to the Poisson statistics in Fig. 4.

distribution for a coherent light source, the Bose-Einstein distribution has $\sigma_n^2 > \bar{n}$, a marking characteristic of thermal light.

As a final remark, we note that in both cases the percentage difference increases with the increase of the afterpulse threshold. This is to be expected since by moving τ_{ap} towards greater values, the percentage of significant statistics (i.e. valid counts) that is being rejected rises and with it the discrepancy between theoretical and experimental value.

6 Conclusions and outlook

In this work we explored a way to distinguish source types by means of their relative photon counting distribution thanks to an experimental setup devised by T. Arecchi. What can now follow is the correct evaluation of the uncertainties of the computed moments and an estimation of the afterpulse probability (as shown for example in [3]).

---

[1] B. E. A. Saleh and M. C. Teich, *Fundamentals of photonics; 2nd ed.*, Wiley series in pure and applied optics (Wiley, New York, NY, 2007).
[2] F. T. Arecchi, Physical Review Letters **15**, 912 (1965).
[3] G. Humer, M. Peev, C. Schaeff, S. Ramelow, M. Stipčević, and R. Ursin, Journal of Lightwave Technology **33**, 3098 (2015).